Upsala J Med Sci 79: 7–17, 1974

A Convection—Diffusion Model of Capillary Permeability with Reference to Single-injection Experiments

BO ÅBERG and JARL V. HÄGGLUND

From the Institute of Physiology and Medical Biophysics, Biomedical Centre, University of Uppsala, Sweden

ABSTRACT

A theoretical model of the transport of neutral molecules across the capillary wall has been developed. The model is applicable to single-injection experiments. The mutual coupling between the diffusion and convection of solute molecules in extracellular pores under the influence of restriction has been considered as responsible for the capillary permeability. The extraction, which is experimentally measurable, and solute flows across the capillary membrane, have been calculated with the continuity equation in the steady state as well as in the case of relaxation phenomena in the membrane-concentration profile due to non-steady-state properties. Explicit equations of the steady-state extraction, suitable for experimental application, are presented, showing the effect of the convection in increasing the capillary permeability and thus in opposing the restriction caused by the solute–membrane interaction. Non-steady-state computations were performed on an analog computer and showed that back transport from the membrane compartment to the blood stream may be partly responsible for the regain of solute molecules which have earlier passed into the capillary wall.

INTRODUCTION

It has been suggested that the transport of lipid-insoluble molecules across the capillary wall occurs through discrete pores with dimensions comparable to those of small molecules (16, 19, 20). The existence of both small and large pores has been discussed (12). The small pores, which are considered to predominate, have in skeletal muscle, for instance, an estimated radius in the range of 3 to 4 nm. Other organs show slightly different values. On the basis of electron-microscopic evidence, it has been proposed that the intercellular junctions are the anatomical counterparts of the small pores (15).

The transport mechanism in the capillary membrane for small molecules has been assumed to be diffusion, modified by a restriction factor due to the finite dimensions of the pores (19, 22). The contribution to the solute flux due to convection (i.e. solvent drag), in accordance with Starling's hypothesis of transcapillary solvent circulation, has usually been treated as a small correction (12, 16).

In experimental investigations of the capillary permeability, what is called the single-injection technique has been widely used (6, 7, 8). In this method, a bolus, containing an impermeable reference substance and permeable test substances, is injected into an afferent artery, and the blood is sampled and analysed at the corresponding efferent vein. By comparing the venous concentrations of the test substances and the reference solute, the amounts of the test substances absorbed can be calculated as an indirect measure of the capillary permeability.

The aim of the present investigation is to study a capillary-membrane model which takes into account the combined effect of convection and diffusion in restricted pores as transcapillary transport mechanisms. The interaction of convection on the diffusion equation has been studied in several other theoretical and experimental situations (11, 13, 14, 17, 21, 23, 24). The present membrane model has been adapted to single-injection experiments by adding a single-channel model of the blood capillary system. Calculations have been made for the steady-state case of the convection–diffusion equation. However, since the time-varying bolus concentration may induce a diffusional non-steady state, this situation is also treated and discussed.

NOMENCLATURE

For convenience, the various notations used throughout the paper are listed as follows. These symbols will also be defined in the text when they appear.

A_p	true pore area (cm²)
A_s	apparent pore area for a solute (cm²)
a	molecular radius (cm)

$c = c(x, t)$	concentration of solute in the blood–tissue barrier as a function of x and t (mole/cm³)
c_n	concentration at intersegmental membrane barrier n (mole/cm³)
$(\partial c/\partial x)_n$	concentration gradient at intersegmental membrane barrier n (mole/cm⁴)
$c_0(t)$	plasma concentration of solute (mole/cm³)
$\hat{c}_0$	maximum plasma solute concentration of the bolus (mole/cm³)
c_d	tissue solute concentration (mole/cm³)
D	diffusion coefficient (cm²/sec)
d	thickness of blood–tissue barrier (cm)
$E(t)$	extraction
E_t	total extraction
$J_s = J_s(x, t)$	solute flow as a function of x and t (mole/(cm² sec))
$(J_s)_n$	solute flow at intersegmental membrane barrier n (mole/(cm² sec))
k	restriction coefficient
N	Avogadro's number (number/mole)
n	index referring to the number of the intersegmental membrane barriers
$P(t)$	permeability of the capillary wall (cm/sec)
P	steady-state capillary permeability (cm/sec)
p	scale factor $= kD/\Delta x^2$
Q	plasma-volume flow (cm³/sec)
q	scale factor $= kv/2\Delta x$
R	gas constant (dyne cm/(mole degree))
r	pore radius (cm)
T	absolute temperature (°K)
t	time (sec)
$t_{1/2}$	half-width of the bolus concentration $c_0(t)$ (sec)
v	linear transendothelial flow velocity (cm/sec)
x	space dimension (cm)
Δx	membrane-segment thickness (cm)
η	viscosity (poise)

The normalized quantities used in this paper have not been included in the above list but are summarized in eq. (9).

MODEL OF THE PLASMA-TISSUE BARRIER

For the transport of neutral lipid-insoluble molecules through the endothelial wall, a pore model has been adopted. Inside the pores, the transport is one-dimensional, and the barrier extends from $x = 0$ on the plasma side to $x = d$ on the interstitial-tissue side of the pores (Fig. 1). A test solute is considered, which for simplicity has a transport rate across the blood-cell membranes which is much slower than both the transport rate across the capillary wall and the transit time of the solute through the capillary system (see the next section). The time-(t)-dependent plasma concentration of this solute is $c_0(t)$, and the membrane concentration is designated $c(x, t)$. The corresponding tissue concentration c_d is assumed to be zero, which means assuming a perfectly stirred extracellular space of infinite extension. The free diffusion coefficient of the solute is D and a constant convection (flow) velocity v is considered to be present within the pores. The solute flux $J_s(x, t)$ in the pores is then:

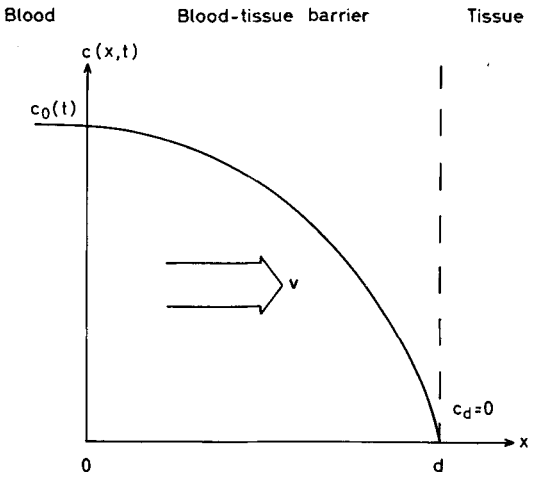

Fig. 1. The convection-diffusion model of the blood-tissue barrier. The convection velocity v disturbs the concentration profile in the membrane of thickness d. The bolus concentration caused by the bolus injection is $c_0(t)$. The tissue concentration c_d is assumed to be zero.

$$J_s(x, t) = -k \cdot D \frac{\partial c(x, t)}{\partial x} + k \cdot v \cdot c(x, t) \qquad (1)$$

where k is the restriction coefficient attributed to the narrowness of the pores. Renkin (cf. 5, 22) assumed that the restriction was caused by a steric hindrance at the entrance of a pore and by frictional forces between the solute and the pore walls. He calculated the restriction coefficient and interpreted it as the apparent pore area A_s for the solute over the true pore area A_p:

$$k = \frac{A_s}{A_p} = \{2(1-a/r)^2 - (1-a/r)^4\}\{1 - 2.104a/r + 2.09(a/r)^3 - 0.95(a/r)^5\} \quad (2)$$

where a/r is the ratio of molecular radius to pore radius. When convection is considered, the frictional forces between the solute and the water must also be taken into account. This was done by Forster (10), who showed that the restriction influences the diffusional and convectional contributions (first and second terms in eq. (1)) in the same proportion. He found that $k = D_{s,m}/(D + D_{s,m})$ where $D_{s,m}$ is the solute-diffusion coefficient against the membrane and D, as above, the value in free solution.

When the transport flux is not in the steady state, the following differential equation, obtained from the continuity equation, describes the concentration within the pores:

$$\frac{\partial c(x,t)}{\partial t} = k \cdot D \frac{\partial^2 c(x,t)}{\partial x^2} - k \cdot v \frac{\partial c(x,t)}{\partial x} \quad (3)$$

Thus, in the non-steady state the concentration is calculated from eq. (3) and the solute flux is then obtained from eq. (1).

Finally, it has been assumed that the solute flux does not influence the plasma concentration $c_0(t)$, which means assuming that the amount of substance lost through the capillary walls is small, as compared with the amount of substance in the plasma, and also that the plasma compartment is well stirred.

MODEL OF THE BLOOD CAPILLARY SYSTEM

In order to adapt the membrane model to single-injection experiments, a model of the blood capillary system is needed to describe the blood flow through the organ under investigation. The simplest model is to approximate the blood capillaries to a single channel (Fig. 2). At the arterial end of the channel, the solute flow from the plasma towards the tissue compartment is $J_s(0, t)$. The water flow with velocity v is thought to be filtered out from the vascular bed at the arterial end and re-absorbed at the venous end, according to Starling's principle of paracapillary circulation. All events in the reabsorptive part, as solute reabsorption from the tissue to the blood or a possible loss of solute from the blood to the tissue are neglected. All the solute flow entering the tissue

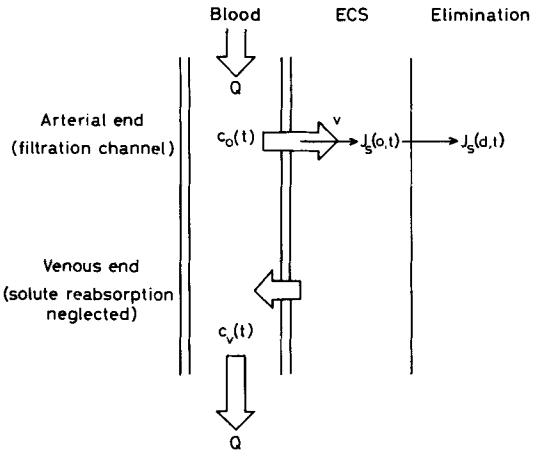

Fig. 2. The four-compartment model of the solute transport from the plasma across the capillary wall to the extracellular space (ECS) and its elimination. The capillary system is modelled by a single channel with a circulating solvent flow v across the endothelial membrane (cf. Fig. 1). See text for further explanation.

compartment, $J_s(d, t)$, can thus be thought of as being eliminated. The volume flow of lymph is usually very small, as compared with the total volume flow of plasma Q in the capillary system, which means that putting the plasma inflow at the arterial end equal to that at the venous end is a good approximation. If the arterial and venous solute concentrations are called $c_0(t)$ and $c_v(t)$ respectively, then a material balance gives

$$Q \cdot c_0(t) = A_p \cdot J_s(0, t) + Q \cdot c_v(t) \quad (4)$$

or

$$c_v(t) = c_0(t) - A_p \cdot J_s(0, t)/Q \quad (5)$$

Calculation of $J_s(0, t)$ from eq. (1), using eq. (3) as described above, thus makes it possible to obtain the experimentally measurable quantity $c_v(t)$ from eq. (5).

EXTRACTION

In single-injection techniques, the experimental result is often expressed as the extraction $E(t)$, which is a measure of the loss of solute into the tissue, as compared with the amount of solute in the bolus (8).

$$E(t) = 1 - \frac{c_v(t)}{c_0(t)} \quad (6)$$

Using the result from eq. (5), we obtain:

$$E(t) = \frac{A_p \cdot J_s(0,t)}{Q \cdot c_0(t)} = \frac{A_p}{Q} P(t) \tag{7}$$

where $P(t)$ is the membrane permeability. This means that in our model the extraction is proportional to the permeability of the capillary wall.

In the experimental situation, the extraction is time-dependent, due to non-steady state phenomena, and different methods of dealing with this situation have been discussed, for instance, the method of calculating the "early extraction" $E(0)$ (18). We have used a different approach by introducing the *total extraction*, defined as

$$E_t = \frac{A_p}{Q} \cdot \frac{\int_0^\infty J_s(0,t)\,dt}{\int_0^\infty c_0(0,t)\,dt} \tag{8}$$

The total extraction E_t means the total loss of solute from the plasma stream, divided by the amount of solute in the injected bolus. In the present model, E_t will vary with the half-width $t_{1/2}$ of the arterial bolus concentration $c_0(t)$, as long as the transport equation (3) is in the non-steady state. In the steady state, the extraction is independent of time, and eq. (8) is reduced to eq. (7).

NORMALIZATIONS

In order to give a comprehensive theoretical description, the following normalizations are introduced:

Normalization table

$$\begin{aligned}
\mathbf{x} &= x/d \\
\mathbf{t} &= t \cdot k \cdot D/d^2 \\
\mathbf{t}_{1/2} &= t_{1/2} \cdot k \cdot D/d^2 \quad \text{(see below)} \\
\mathbf{c}_0(\mathbf{t}) &= c_0(t)/\hat{c}_0 \\
\mathbf{c}_v(\mathbf{t}) &= c_v(t)/\hat{c}_0 \\
\mathbf{v} &= v \cdot d/D \\
\mathbf{V} &= v \cdot d \cdot r \cdot 6\pi \cdot \eta \cdot N/RT \quad \text{(see below)} \\
\mathbf{J_s(x,t)} &= J_s(x,t) \cdot d/(k \cdot D \cdot \hat{c}_0) \\
\mathbf{E} &= \frac{E(t) \cdot d \cdot Q}{k \cdot D \cdot A_p} = \frac{P(t) \cdot d}{k \cdot D} \quad \text{and} \\
\mathbf{E_t} &= \frac{E_t \cdot d \cdot Q}{k \cdot D \cdot A_p}
\end{aligned} \tag{9}$$

where $\hat{c}_0$ is the maximum of $c_0(t)$. $\mathbf{v}$ denotes the convection velocity v divided by the diffusional velocity obtained with zero convection. Correspondingly, $\mathbf{J_s(x,t)}$ is the ratio of the solute flux and the maximum diffusional flux (without convection). $\mathbf{E}$ and $\mathbf{E_t}$, can be interpreted as the extraction or total extraction divided by the extraction obtained from pure diffusion. The normalized extraction $\mathbf{E}$ is equal to the permeability $P(t)$ normalized to the permeability with only diffusion. These relations are easily established if we consider that $J_s(0,t)/c_0(t) = kD/d$ in the case of pure diffusion and use eq. (7).

STEADY-STATE APPROXIMATION

The calculations are substantially simplified if the approximation to the steady-state transport equation is made, which means neglecting the time derivative in eq. (3) ($\partial/\partial t = 0$). Since $c_0(t)$ varies with time, $c(x,t)$ will vary with time also in the steady-state approximation, but the variation of $c_0(t)$ in this approximation is much slower than the relaxation time of eq. (3). The validity of this steady-state approximation will be further discussed below.

Using the normalizations introduced in the preceding section and assuming the steady-state condition, eqs. (1), (3) and (7) (or (8)) are transformed into

$$\mathbf{J_s(x,t)} = -\partial \mathbf{c(x,t)}/\partial \mathbf{x} + \mathbf{v} \cdot \mathbf{c} \tag{10}$$

$$\frac{\partial^2 \mathbf{c(x,t)}}{\partial \mathbf{x}^2} = \mathbf{v} \frac{\partial \mathbf{c(x,t)}}{\partial \mathbf{x}} \tag{11}$$

and

$$\mathbf{E} = \mathbf{J_s(0,t)}/\mathbf{c_0(t)} \tag{12}$$

Eqs. (10) and (12) are valid also in the non-steady state, but eq. (11) includes the steady-state approximation.

The *boundary conditions* of eq. (11) can be expressed in normalized quantities, such as (cf. Fig. 1)

$$\mathbf{c(0,t)} = \mathbf{c_0(t)} \quad \text{and} \qquad \mathbf{c(1,t)} = 0 \tag{13}$$

The differential equation (11) is easily solved, together with the boundary conditions (eq. (13)), and the expression $\mathbf{c(x,t)}$ is then used in eq. (10), which, in combination with eq. (12), gives an expression of the extraction $\mathbf{E}$. The details of this procedure are given in the Appendix and the result is (eq. (A7)):

$$\mathbf{E} = \frac{\mathbf{v}}{1 - \exp(-\mathbf{v})} \tag{14}$$

A graphical representation of eq. (14) (continuous curve) is given in Fig. 3. The inset diagram in Fig. 3 shows the relation between v and the concentration profile within the plasma-tissue membrane, as calculated from eq. (A5) in the Appendix. The figure illustrates that, as expected, the convection increases the extraction. At high filtration rates, the convection term predominates over the diffusion and the extraction approaches proportionality with v.

In experimental work, using the single-injection technique, the ratio of the capillary-wall permeability and the free diffusion coefficient of the solute has been used to express the transport properties of the blood tissue barrier (2). In the present model, the corresponding quantity can be given as the actual permeability P divided by the permeability of free diffusion (D/d), a ratio which is proportional to the ratio of the extraction $E(t)$ and the free diffusion coefficient D. Then from eqs. (9) and (14):

$$P \cdot d/D = E(t) \cdot d \cdot Q/(D \cdot A_p) = k \frac{\mathrm{v}}{1 - \exp(-\mathrm{v})} \qquad (15)$$

This expression is illustrated in Fig. 4 (continuous curves) with k calculated from eq. (2). Different solute molecules correspond to different values of the molecule-to-pore radius a/r, but also to different v, since the free diffusion coefficient which varies with the molecular size, is included in the normalization ($\mathrm{v} = vd/D$).

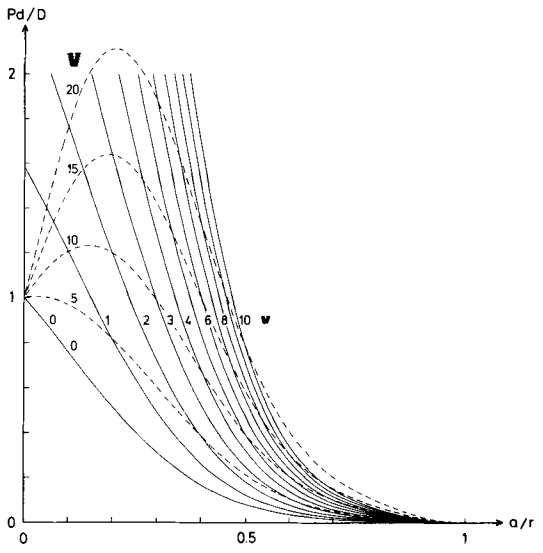

Fig. 4. The ratio of steady-state capillary permeability P and the free diffusion permeability D/d as a function of the solute- to molecular-radius ratio for various values of the convection velocity v (——) and V (– – –). The ordinate is proportional to the extraction divided by the free diffusion coefficient. On the constant V curves, the convection velocity v is constant, while the molecular radius varies according to the abscissa. It will be seen that for a certain value of v different molecules correspond to different values of v and subsequently to different shapes of the capillary membrane-concentration profile (cf. the inset diagram in Fig. 3).

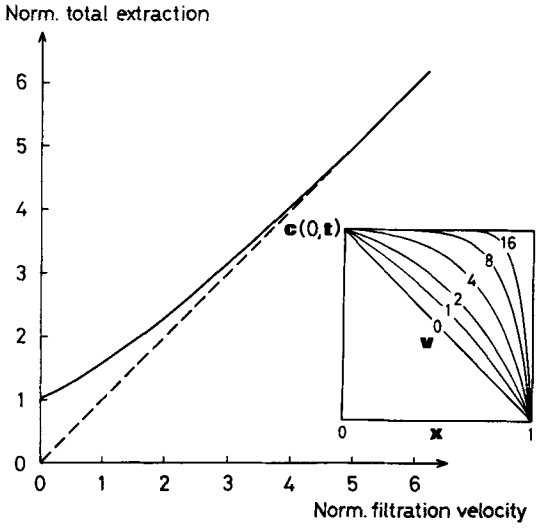

Fig. 3. The steady-state extraction E as a function of the covection velocity v (continuous curves). The inserted diagram shows the concentration profiles in the capillary membrane corresponding to different v-values. Note that $\mathrm{v} = 0$ correspond to pure diffusion and that for high values of v the extraction is proportional to v, indicating a negligible contribution by diffusion to the transcapillary transport.

If we introduce the Stoke–Einstein relation between the free diffusion coefficient and the molecular radius (a), an experimentally more convenient expression of the permeability is obtained:

$$D = RT/(6\pi \cdot \eta \cdot N \cdot a) \qquad (16)$$

where R = the gas constant, T = the absolute temperature, η = the viscosity and N = Avogadro's number. Then, from eqs. (9), (15) and (16) we have

$$P \cdot d/D = k \frac{\mathrm{V}(a/r)}{1 - \exp(-\mathrm{V}a/r)} \qquad (17)$$

Eq. (17) is illustrated in Fig. 4 by dashed curves. In an experiment with constant convection velocity v but different probe molecules, the results will fall on one of these constant V curves. Such an experiment may thus give rise to (a) increasing, (b) approximately constant or (c) decreasing values of Pd/D as

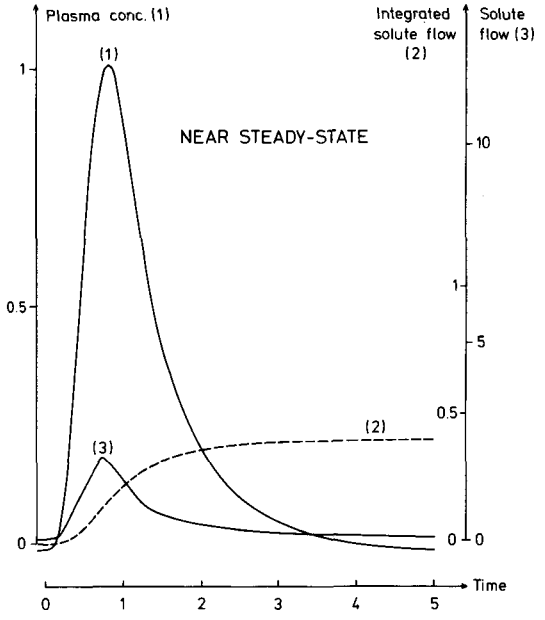

Fig. 5. The plasma solute concentration $\mathbf{c_0(t)}$ caused by a single injection, the solute flow $\mathbf{J_s(0, t)}$ across the capillary wall and the integrated solute flow $\int_0^t \mathbf{J_s(0, t)}\, dt$ as functions of time **t**. The integrated solute flow represents the instantaneous absorption from the plasma. The curves were calculated by analog computation and are given for $\mathbf{v = 1}$ and for $\mathbf{t_{1/2} = 0.9}$, which means an *almost steady-state* condition. Note that the solute flux (curve (3)) at each time is almost proportional to the plasma concentration (cruve (1)) in this case.

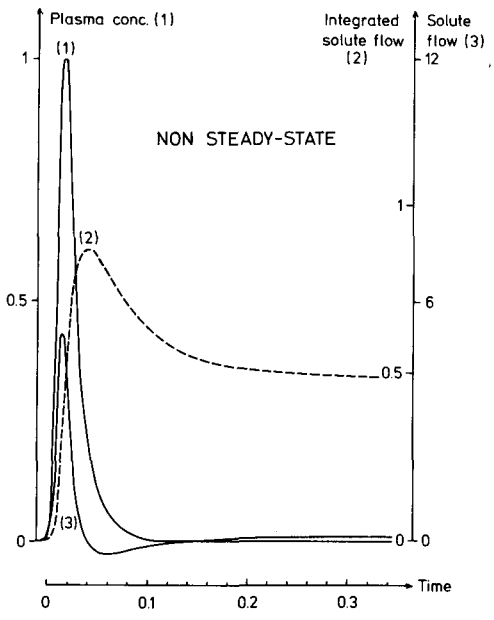

Fig. 6. The same as Fig. 5 but for $\mathbf{t_{1/2} = 0.02}$, which means that the transport equation is in the *non-steady state*. In this case, there is a back transport from the capillary membrane to the plasma (curve (3)) during the descending part of the plasma solute concentration (curve (1)). This is also reflected in the fact that the integrated solute flow is descending at the same time.

a function of a/r. In other words, the consequence of convection is to oppose the restriction, but finally with increasing molecular size the restriction will predominate and reduce the permeability towards zero.

NON-STEADY-STATE CALCULATIONS

When the time relaxation of the concentration profile within the capillary wall is appreciable, as compared with the time course of the bolus concentration $c_0(t)$, the complete diffusion equation must be solved (eqs. (3) and (9)).

$$\frac{\partial \mathbf{c(x, t)}}{\partial \mathbf{t}} = \frac{\partial^2 \mathbf{c(x, t)}}{\partial \mathbf{x}^2} - \mathbf{v}\frac{\partial \mathbf{c(x, t)}}{\partial \mathbf{x}} \qquad (18)$$

This equation, together with the appropriate boundary conditions according to eq. (13), and eq. (10), have been solved by means of analog computations. The bolus concentration $c_0(t)$ was taken from a single-injection experiment as the venous concentration of an essentially non-permeable solute, namely, Evans blue bound to albumin (1). This curve corresponds to the so-called lagged normal density curve in indicator–dilution experiments (3). The bolus concentration was generated on a function generator, and the degree of non-steady state was simulated by varying the time width $t_{1/2}$ at half the maximum value of the bolus concentration, i.e. at $c_0(t) = \hat{c}_0/2$ (4).

The method of the analog solution was to use a finite-difference approximation of the equations, as described in more detail in the Appendix. The analog computer used was a Donner 3000 and the results were recorded on a servo recorder three-channel Watanabe Multicorder, model H.S.

Figs. 5 and 6 show the results for $\mathbf{v = 1}$ and for two values of the half-width, $\mathbf{t_{1/2} = 0.9}$ and $\mathbf{t_{1/2} = 0.02}$ respectively, corresponding to an almost steady-state condition (Fig. 5) and to the non-steady state (Fig. 6). The solid curves are the bolus concentration $\mathbf{c_0(t)}$ and the solute flow $\mathbf{J_s(0, t)}$ across the capillary wall, and the dashed curves are the integrated solute

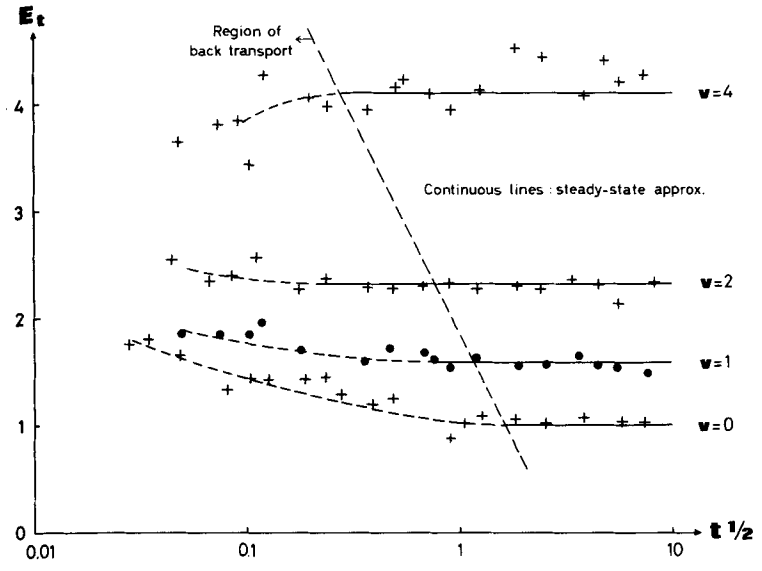

Fig. 7. The total extraction E_t as a function of $t_{1/2}$ for different values of the convection velocity v. The dots and crosses were obtained from analog computations, and the continuous lines from the steady-state approximation (Eq. (14) and Fig. 3). Back transport (cf. Fig. 6) occurs approximately to the left of the oblique dashed line.

flow at each instant, $\int_0^t J_s(0, t)dt$. For the steady-state case (Fig. 5), the solute flux is proportional to the bolus concentration and the extraction can easily be calculated from eq. (12). On the other hand, in the non-steady state, there is non-proportionality corresponding to a non-constant extraction during the passage of the bolus. Furthermore, at the latter part of the bolus the solute is transported back to the plasma from the accumulated solute in the plasma-tissue membrane. This phenomenon, which is associated with non-steady-state behaviour, will in the following text be called *back transport*, in contrast to the term *re-absorption*, which we shall connect with the transport of solute from the extracellular space back to the plasma compartment. As already mentioned, the re-absorption was neglected in the present model by assuming zero tissue concentration.

Finally, the total extraction was calculated for different values of $t_{1/2}$ and v, according to the equation (see eqs. (8) and (9))

$$E_t = \frac{\int_0^\infty J_s(0, t)\,dt}{\int_0^\infty c_0(0, t)\,dt} \qquad (19)$$

using the analog procedure already mentioned. The results are summarized in Fig. 7, and illustrate that high values of $t_{1/2}$ correspond to the steady-state approximation, eq. (14) and Fig. 3, and that small $t_{1/2}$ values imply the non-steady state. The transition region between the validity of the steady-state approximation and the non-steady-state condition is roughly given by the oblique dashed line, to the left of which back transport is obtained. It will be seen that this transition occurs where $t_{1/2}$ is of the order of 1, which is also to be expected from the normalized diffusion equation (eq. (18)).

DISCUSSION

The validity of the model

The models of the capillary permeability and the blood-capillary spatial distribution are, of course, somewhat oversimplified, as compared with the actual biological situation. At the membrane level, for instance, the possibility of unstirred layers in the plasma as well as in the extracellular space (9) have not been included. The assumption of zero tissue concentration, $c_d = 0$, means neglecting the effect of gradients in the tissue space and disregarding the re-absorption back to the blood capillary from the tissue and the exchange between capillaries. The validity of the approximation of zero extracellular concentration is thought to be better at the beginning of the venous outflow curves, and also better for larger molecules, which pass through the capillary wall at a relatively slow rate.

Furthermore, the distribution of the pore geometry, as concerns radius, length and tortuousness, has not been treated, nor has the distribution of the convection velocity. The pore radius and convec-

tion velocity should therefore be regarded as average values of a more complicated situation.

The shape of $c_0(t)$ at the pores is supposed to be fairly well described by the lagged normal density curve (3), but in a biological capillary net there is certainly a distribution of transit times (4) which complicates the absorption from the blood and the exchange properties between the capillaries.

Experimental applicability of the model

The main features of the present model are the assumption of a significant convectional flow across the endothelial wall and the introduction of the concept of the non-steady state, with relaxation of the membrane-concentration profile during the passage of the bolus in single-injection experiments. These features may be subject to experimental tests, using the model.

In the diffusional non-steady state, it has been shown that during the latter part of the venous outflow curves there is a back transport from the membrane compartment to the plasma compartment (Fig. 6). This back transport may in many experimental situations be difficult to distinguish from the re-absorption from the extracellular space back to the plasma, a phenomenon which was neglected in the present model. As mentioned above, the non-steady state is roughly obtained when $\mathbf{t}_{1/2} < 1$ and the steady state when $\mathbf{t}_{1/2} > 1$ (Fig. 7). Considering that $\mathbf{t}_{1/2} = t_{1/2}\, kD/d^2$ (eq. (9)), it will be seen that the steady state is likely to occur for small molecules with a high restriction factor k (eq. (2)) and a high value of the free-diffusion coefficient D (eq. (16)). Another important consequence is that the non-steady state seemingly occur for large molecules with sufficiently small D and k values. Thus, the experimental situation may roughly be covered by the following three categories: (a) small molecules probably means a fast steady-state transport with relatively early re-absorption, (b) medium molecules mean the steady state with re-absorption appearing later, and (c) large molecules imply the non-steady state and negligible re-absorption. One method of investigating these possibilities would be to use different test molecules. It has been shown that for glucose and raffinose, the extraction is constant, with respect to time, over the main part of the venous-outflow curves, which means that these molecules fit well in the second category above (1).

The possibility of the non-steady state may be further illustrated by the following numerical example. Assuming $t_{1/2} = 1$ sec, $k = 0.1$ ($a/r = 0.5$) and $D = 10^{-6}$ cm^2/sec and using the relation $t_{1/2}\, kD/d^2 < 1$, we find that $d > 3$ μm is a condition for the non-steady state. It may be mentioned that Pappenheimer considered the microscopic thickness of the capillary wall to be between 0.1 and 1 μm (19). As mentioned above, however, the membrane thickness d may be increased by the presence of unstirred layers at the blood capillary wall and in the extracellular space.

The constancy of the extraction over a major part of the venous concentration curve may be considered as a pre-requisite for the use of the steady-state equations. For this case, the convection velocity v can be estimated from Fig. 4, using several probe molecules with constant or maybe also different values of v.

Appendix

Steady-state solution

The steady-state approximation is described by eqs. (10)–(13):

$$\frac{\partial^2 \mathbf{c}(\mathbf{x}, \mathbf{t})}{\partial \mathbf{x}^2} = \mathbf{v}\, \frac{\partial \mathbf{c}(\mathbf{x}, \mathbf{t})}{\partial \mathbf{x}} \qquad \text{(A1)} = \text{(11)}$$

Boundary conditions

$$\mathbf{c}(0, \mathbf{t}) = \mathbf{c}_0(\mathbf{t}) \quad \text{and} \qquad \text{(A2)} = \text{(13)}$$

$$\mathbf{c}(1, \mathbf{t}) = 0$$

$$\mathbf{J}_s(\mathbf{x}, \mathbf{t}) = -\partial \mathbf{c}(\mathbf{x}, \mathbf{t})/\partial \mathbf{x} + \mathbf{v} \cdot \mathbf{c} \qquad \text{(A3)} = \text{(10)}$$

$$\mathbf{E} = \mathbf{J}_s(0, \mathbf{t})/\mathbf{c}_0(0, \mathbf{t}) \qquad \text{(A4)} = \text{(12)}$$

The solute concentration inside the plasma–tissue membrane is obtained by solving the differential equation (A1), together with the boundary conditions (eq. (A2)), which gives

$$\mathbf{c}(\mathbf{x}, \mathbf{t}) = \frac{e^{\mathbf{vx}} - e^{\mathbf{v}}}{1 - e^{\mathbf{v}}}\, \mathbf{c}_0(\mathbf{t}) \qquad \text{(A5)}$$

Now combining eqs. (A5) and (A3) gives the solute flux

$$\mathbf{J}_s(\mathbf{x}, \mathbf{t}) = \frac{\mathbf{v}}{1 - \exp(-\mathbf{v})}\, \mathbf{c}_0(\mathbf{t}) \qquad \text{(A6)}$$

which is independent of $\mathbf{x}$.

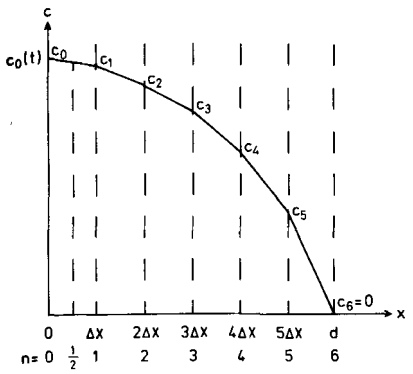

Fig. 8. The convection-diffusion model of the solute transport across the capillary wall, as approximated for analog computation (cf. Fig. 1). The plasma–tissue barrier is divided into 6 segments, each Δx wide. The finite-difference method means straight-line approximation of the concentrations within the segments.

Finally, the extraction is obtained from eqs. (A6) and (A4):

$$\mathbf{E} = \frac{\mathbf{v}}{1 - \exp(-\mathbf{v})} \qquad \text{(A7)} = \text{(14)}$$

Non-steady-state computations

The non-steady-state solutions were obtained by means of analog computations. The non-normalized equations were used for this case. Normlized equations can be solved with equal ease but need the introduction of time-scaling, which is implicit in the non-normalized solution. The solute concentration $c = c(x, t)$ and solute flux $J_s = J_s(x, t)$ within the plasma–tissue membrane are given by the following equations:

$$\frac{\partial c(x,t)}{\partial t} = k \cdot D \frac{\partial^2 c(x,t)}{\partial x^2} - k \cdot v \frac{\partial c(x,t)}{\partial x} \qquad \text{(A8)} = \text{(3)}$$

Boundary conditions

$$c(0, t) = c_0(t) \quad \text{and}$$
$$c(d, t) = 0 \qquad \text{(A9)} = \text{(13)}$$

$$J_s(0, t) = -k \cdot D \frac{\partial c}{\partial x} + k \cdot v \cdot c \qquad \text{(A10)} = \text{(1)}$$

To solve these equations on an analog computer, a conventional finite-difference approximation method was adopted. The plasma–tissue barrier was divided into six segments of thickness Δx, as shown in Fig. 8. The first- and second-order derivatives with respect to x of the concentration c_n at intersegmental barriers of number n can be expressed as

$$(\partial c/\partial x)_n = (c_{n+1} - c_{n-1})/2\Delta x \quad \text{for} \quad n = 1, 2, \ldots 5 \qquad \text{(A11)}$$

$$(\partial c/\partial x)_{n-1/2} = (c_n - c_{n-1})/\Delta x \quad \text{for} \quad n = 1, 2, \ldots 6 \qquad \text{(A12)}$$

$$(\partial^2 c/\partial x^2)_n = (c_{n+1} - 2c_n + c_{n-1})/\Delta x^2 \quad \text{for}$$
$$n = 1, 2, \ldots 5 \qquad \text{(A13)}$$

The insertion of eqs. (A11)–(A13) in eqs. (A8)–(A10) and approximating $J_s(0, t)$ by the solute flow $(J_s)_{1/2}$ at $n = 1/2$ yields

$$\partial c/\partial t = p(c_{n+1} - 2c_n + c_{n-1}) - q(c_{n+1} - c_{n-1}) \qquad \text{(A14)}$$

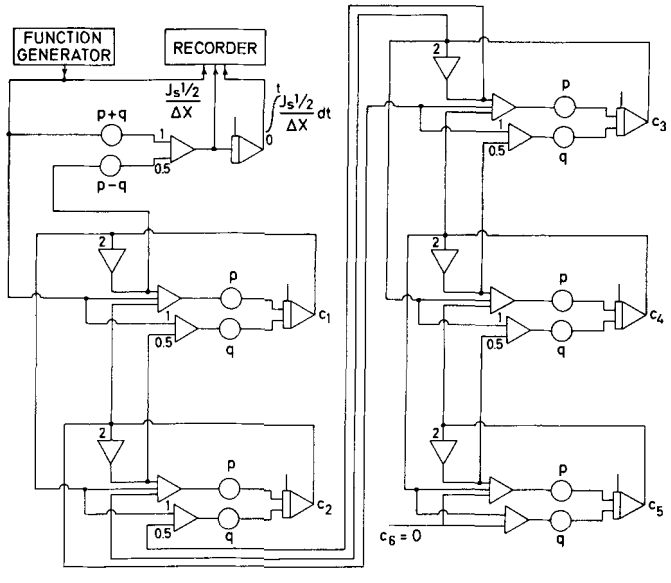

Fig. 9. Analog-computer diagram for the model in Fig. 8, derived from eqs. (A14)–(A18). The function generator was used to simulate the plasma solute concentration $c_0(t)$. The parameters p and q (eq. (A 16)) were adjusted on precision potentiometers.

Boundary conditions

$$c_0 = c_0(t) \quad \text{and}$$

$$c_6 = 0 \tag{A15}$$

$$(J_s)_{1/2}/\Delta x = (p+q)c_0 - (p-q)c_1 \tag{A16}$$

where the following parameters were introduced:

$$p = k \cdot D/\Delta x^2 \tag{A17}$$

and

$$q = k \cdot v/2\Delta x \tag{A18}$$

The relations between the normalized values of the convection velocity and of the half-bolus time width, on the one hand, and of the parameters p and q, on the other hand, are given by

$$\mathbf{v} = 12q/p \tag{A19}$$

and

$$\mathbf{t}_{1/2} = t_{1/2} \cdot p/36 \tag{A20}$$

Eqs. (A14)–(A18) are suitable for analog programming, and the analog-computer diagram of these equations which was used is shown in Fig. 9. For the calculations, the following initial conditions were applied to the computer:

$$c_n = 0 \quad \text{at} \quad t < 0 \quad \text{for} \quad n = 0, 1, \ldots 5 \tag{A21}$$

The degree of the non-steady state was varied by changing the parameter p (eq. (A20)), and the convection velocity was then chosen by the parameter q, according to eq. (A19).

ACKNOWLEDGEMENTS

The authors are greatly indebted to Professor T. Teorell for initiating this work and for much valuable advice and many stimulating discussions. We also wish to thank Miss C. Ferner for valuable technical assistance.

This work was supported by grants from the Medical Faculty of the University of Uppsala, the Swedish Medical Research Council (Project No. 14X-629) and the National Institutes of Health (Grant No. 5 R01 HE 12960-08).

REFERENCES

1. Åberg, B.: Manuscript in preparation. 1974.
2. Alvarez, O. A. & Yudilevich, D. L.: Heart capillary permeability to lipid-insoluble molecules. J Physiol (London) *202:* 45, 1969.
3. Bassingthwaighte, J. B., Ackerman, F. H. & Wood, E. H.: Applications of the lagged normal density curve as a model for arterial dilution curves. Circ Res, *18:* 398, 1966.
4. Bassingthwaighte, J. B.: Plasma indicator dispersion in arteries of the human leg. Circ Res *19:* 332, 1966.
5. Beck, P. E. & Schultz, J. S.: Hindered diffusion in microporous membranes with known pore geometry. Science *170:* 1302, 1970.
6. Chinard, F. P., Vosburgh, G. J. & Enns, T.: Transcapillary exchange of water and other substances in certain organs of the dog. Am J Physiol *183:* 221, 1955.
7. Crone, C.: Om diffusionen av nogle organiske nonelektrolyter fra blod til hjernevæv. (Thesis). Munksgaard, København, 1961.
8. — The permeability of capillaries in various organs as determined by use of the "indicator diffusion" method. Acta Physiol Scand. *58:* 292, 1963.
9. Crone, C. & Garlick, D.: The penetration of inulin, sucrose, manitol and tritiated water from the interstitial space in muscle into the vascular system. J Physiol (London) *210:* 387, 1970.
10. Forster, R. E.: The transport of water in erythrocytes. *In* Current Topics in Membranes and Transport (ed. F. Bronner & A. Kleinzeller), Vol. 2, pp. 41–98. Academic Press, New York, 1971.
11. Garby, L.: Studies on transfer of matter across membranes with special reference to the isolated human amniotic membrane and the exchange of amniotic fluid. Acta Physiol Scand, Suppl. *137,* 1957.
12. Grotte, G.: Passage of dextran molecules across the blood-lymph barrier. Acta Chir Scand, Suppl. *211,* 1956.
13. Hertz, G.: Über Trennung von Gasgemischen durch Diffusion in einem strömenden Gase. Z. Physik *19:* 35, 1923.
14. Jacobs, M. H.: Diffusion processes. Ergebn Biol. *12:* 1, 1935.
15. Karnovsky, M. J.: The ultrastructural bases of transcapillary exchange. *In* Biological Interfaces: Flows and Exchanges. Little, Brown & Co., Boston, 1968.
16. Landis, E. M. & Pappenheimer, J. R.: Exchange of substances through the capillary walls. *In* Handbook of Physiology, Sect. 2: Circulation (ed. W. F. Hamilton), Vol. II, pp. 961–1034. Amer. Physiol. Soc., Washington, D.C., 1963.
17. Manegold, E. & Solf, K.: Über Kapillarensysteme, XIV. 1. Die Dynamik osmotischer Zellen. Kolloid Z *54:* 179, 1932.
18. Martin, P. & Yudilevich, D.: A theory for the quantification of transcapillary exchange by tracer-dilution curves. Am J Physiol *207:* 162, 1964.
19. Pappenheimer, J. R., Renkin, E. M. & Borrero, L. M.: Filtration, diffusion and molecular sieving through peripheral capillary membranes. A contribution to the pore theory of capillary permeability. Am J Physiol *167:* 13, 1951.
20. Pappenheimer, J. R.: Passage of molecules through capillary walls. Physiol Rev *33:* 387, 1953.
21. Rapoport, S. I.: Ionic accumulation by water flow through a membrane. Acta Physiol Scand *64:* 361, 1965.
22. Renkin, E. M.: Filtration, diffusion, and molecular sieving through prorous cellulose membranes. J Gen Physiol *38:* 225, 1954.

23. Teorell, T.: Zur quantitativen Behandlung der Membranpermeabilität. Z Elektrochem *55:* 460, 1951.
24. — General physico-chemical aspects of drug distribution. *In* Advances in the Biosciences 5 (ed. G. Raspé), pp. 21–37. Pergamon Press, Oxford, 1969.

Received September 14, 1973

Adress for reprints:

Bo Åberg
Inst. of Physiology and Medical Biophysics
Bio-Medical Center
Box 572
S-751 23 Uppsala
Sweden